



Activity and thermal stability of Rh-based catalytic system for an advanced modern TWC

Iljeong Heo^a, Dal Young Yoon^a, Byong K. Cho^a, In-Sik Nam^{a,*}, Jin Woo Choung^b, Seungbeom Yoo^b

^a School of Environmental Science and Engineering/Department of Chemical Engineering, Pohang University of Science and Technology (POSTECH), San 31 Hyoja-Dong, Pohang, 790-784, Republic of Korea

^b Exhaust Emission Engineering Team, Research & Development Division, Power Train R&D Center, Hyundai Motor Company, 772-1 Jangduk-Dong, Hwaseong, 445-706, Republic of Korea

ARTICLE INFO

Article history:

Received 2 January 2012
Received in revised form 28 March 2012
Accepted 28 March 2012
Available online 5 April 2012

Keywords:

TWC
Rh/ZrO₂
Catalyst deactivation
NH₃ formation
TWC monolith

ABSTRACT

The catalytic activity and thermal durability of Rh supported on a variety of metal oxides for removing NO_x in the three-way catalyst (TWC) converter have been investigated under realistic gasoline engine exhaust conditions. Among the Rh/metal oxide catalysts examined, the Rh/ZrO₂ catalyst has the best thermal durability. The catalytic activity and thermal stability of the Rh/ZrO₂ catalysts have shown strong dependence on the ZrO₂ support employed, with the ZrO₂ prepared by the sol–gel (SG) and precipitation (P) methods exhibiting the most favorable catalytic performance. The improved TWC performance and thermal stability of the Rh/ZrO₂ (SG and P) catalysts compared to other Rh/ZrO₂ catalysts are mainly due to the structural difference in the underlying ZrO₂ supports. Both ZrO₂ (P) and ZrO₂ (SG) contain the tetragonal as well as the monoclinic phase of ZrO₂, whereas the others are primarily in the monoclinic phase. Deactivation of the Rh/ZrO₂ upon thermal aging is mainly caused by the loss of the active metal surface area of Rh due to sintering and/or burial of Rh into the sublattice of ZrO₂. The strong interaction of Rh with the tetragonal phase of ZrO₂ appears to prevent the burial of Rh into ZrO₂ lattice during the thermal aging. A series of comparative kinetic experiments revealed that the Rh/ZrO₂ (SG and P) catalysts among other Rh/metal oxide catalysts produce the least amount of harmful NH₃, which can be subsequently oxidized to hazardous NO_x over the Pd-based oxidation catalyst co-existing in the TWC converter. A dual-brick monolith system washcoated with Rh/ZrO₂ (P) and Pd/Al₂O₃ in the front and the rear bricks, respectively, has shown superior thermal durability over monolith configurations investigated in the present study.

© 2012 Elsevier B.V. All rights reserved.

1. Introduction

The three-way catalyst (TWC) converter, which has been in active use since 1975, is the most effective catalytic system for removing air pollutants, including CO, HCs and NO_x, emitted from gasoline engines operating under the stoichiometric condition [1,2]. To meet the worldwide stringent automotive emission regulations, the TWC requires a large amount of highly active noble metals (NM) including Pt, Pd and Rh supported on metal oxides with high surface areas. Pt and Pd have long been the active components for the oxidation of CO and HCs, while Rh has been known to be active for the reduction of NO_x during the course of the TWC reactions [1]. Since Pd has emerged as an appropriate substitute for Pt for economic reasons, the commercial modern TWC includes the Pd/Rh bimetallic catalytic system to simultaneously remove CO, HCs and NO_x, instead of the Pt/Rh system [2]. Alumina has been

regarded as the best catalyst support for TWC, mainly due to its pertinent properties and the reason for the cost reduction [1]. Additional ingredients such as ceria and zirconia also play an important role as a catalyst promoter to further enhance the TWC performance and durability [2,3].

Recently, Pd/ and/or Rh/alumina catalysts containing promoters have been widely employed in commercial modern TWC systems to remove CO, HCs and NO_x simultaneously [1]. Since TWCs typically operate at high exhaust gas temperature, the catalysts are prone to deactivation due to the sintering of NMs and the formation of an alloy between NMs themselves as well as thermal degradation of another catalyst component including catalyst support [4–6]. In particular, the phase of Rh supported on alumina readily forms Rh aluminate under a high temperature oxidizing environment due to the fuel cut control of the modern gasoline engine, resulting in the loss of its NO_x reduction activity [7,8]. Yao et al. [9] reported that the Rh aluminate formed below 700 °C is reversibly transformed back to the independent metallic Rh and alumina phases by the reductive treatment with H₂ at a temperature higher than 550 °C. However, once the Rh is incorporated into alumina at 900 °C under

* Corresponding author. Tel.: +82 54 279 2264; fax: +82 54 279 8299.
E-mail address: isnam@postech.ac.kr (I.-S. Nam).

Table 1
Physical properties of Rh/metal oxide catalysts.

Catalyst	Rh content (wt.%)		BET surface area (m ² /g)		Active metal area (m ² _{Rh} /g _{catalyst})		Supports
	Fresh	Aged	Fresh	Aged	Fresh	Aged	
Rh/Al ₂ O ₃	0.16	0.18	104	17	0.194	0.011	γ-Al ₂ O ₃ (commercial)
Rh/SiO ₂	0.17	0.18	31	7	0.044	0.013	SiO ₂ (commercial)
Rh/CeO ₂ (P)	0.18	0.17	42	<5	0.301	0.045	CeO ₂ (precipitation)
Rh/C ₃ Z ₁ (CP)	0.16	0.17	35	<5	0.476	0.038	Ce _{0.75} Zr _{0.25} O ₂ (co-precipitation)
Rh/ZrO ₂ (P)	0.16	0.17	42	9	0.457	0.133	ZrO ₂ (precipitation)

oxidative conditions, the restoration of metallic Rh from the Rh aluminate hardly occurs by the reductive treatment [9]. They also observed that the phase of Rh supported on ZrO₂ is thermally stable, as determined by the CO chemisorption method, and the activity of the Rh/ZrO₂ catalyst for the NO + H₂ reaction is hardly decreased by the thermal aging at 950 °C. ZrO₂ may then be regarded as a promising candidate for the catalyst support, since it not only moderates the growth rate of Rh by sintering but also prevents the formation of the inactive Rh phase such as Rh aluminate [9].

Superior thermal stabilities of Rh/metal oxides have also been reported elsewhere [10–12]. Haneda et al. [10] observed that the Rh/ceria and Rh/cerium zirconium mixed oxide (CZ) with the Ce/Zr ratio of 3 maintained their catalytic activity for removing NO with C₃H₆ even after thermal aging at 1000 °C for 25 h. Moreover, it was reported that Ce moderated the sintering of NM including Pt, mainly due to the strong interaction of Pt–Ce sharing an O atom [13]. Since the CZ is capable of preventing the NM particles from sintering at elevated temperatures, it may also be an alternative support to Al₂O₃ for stabilizing Rh during the thermal aging [10,12,13].

In the present study, the deterioration of the TWC activity over the Rh catalysts supported on a variety of metal oxides by oxidative thermal aging has been systematically examined by using a light-off activity test (LOT) conducted at a slightly lean condition of the realistic exhaust stream of the gasoline engine [5]. In particular, the effect of thermal aging on the alteration of physico-chemical properties of the Rh supported on various ZrO₂ catalysts has been extensively investigated by a variety of the catalyst characterization methods including CO chemisorption, N₂ adsorption, temperature-programmed reduction (TPR), X-ray diffraction (XRD), X-ray photoelectron spectroscopy (XPS), etc. Finally, the feasibility of Rh/ZrO₂ as a deNO_x catalyst in the TWC system has been investigated using a monolith catalyst comprised of Rh/ZrO₂ (P) and the Pd/Al₂O₃ catalysts.

2. Experimental

2.1. Catalyst preparation

ZrO₂, CeO₂ and Ce_{0.75}Zr_{0.25}O₂ were prepared by the sol–gel (SG), precipitation (P) and co-precipitation methods, respectively, while γ-Al₂O₃ (Alfa Aesar) and SiO₂ (Fuji Silysia Chem. Ltd.) were commercial products. Details of the support preparation methods can be found elsewhere [14–16]. Since the ZrO₂ (SG), γ-Al₂O₃ and SiO₂ supports showed weight losses during a heat treatment up

to 700 °C, all metal oxide supports were pre-calcined at 700 °C for 5 h in a muffle furnace to stabilize the supports employed. Then, 0.18 wt.% of Rh was loaded onto those metal oxides by the incipient wetness method. The as-prepared catalysts were then dried at 110 °C followed by calcination at 500 °C for 5 h in static air.

The prepared catalysts were aged at 1000 °C for 20 h in a muffle furnace under the static air condition [17]. The aged catalysts were denoted as “a-” in front of the abbreviations of the catalysts. For example, “a-Rh/ZrO₂” stands for the 0.18 wt.% Rh/ZrO₂ catalyst aged at 1000 °C, while “Rh/Al₂O₃” indicates fresh Rh/Al₂O₃ catalyst containing 0.18 wt.% of Rh before aging. Details of the catalysts employed in the present study are in Tables 1 and 2.

2.2. Catalyst washcoating

The Rh/ZrO₂ (P) and/or Pd/γ-Al₂O₃ catalysts were washcoated onto a cylindrical cordierite monolith substrate (400 cpsi, 5/8 in. (D) × 1 in. (L)) by the conventional dipping method [18]. Note that the Pd/Al₂O₃ catalyst prepared by the impregnation method was employed as the oxidation catalyst in the TWC monolith system. Prior to the dipping step, the catalyst powder and an appropriate amount of distilled H₂O were mixed together and ball-milled with ZrO₂ balls for 72 h to ensure the particle size of the catalyst powder was smaller than 5 μm [19]. Upon completion of the ball-milling, the ZrO₂ balls and catalyst slurry were separated, and the monolith substrates were vertically submerged into the catalyst slurries. A compressed air stream was used to blow out excess washcoating from the monolith channels and external walls of the substrate. The wet monoliths coated with the catalyst slurry were dried in an oven at 120 °C for 1 h. These dipping and drying procedures were repeated until the desired amounts of the catalyst slurry were coated onto the monolith substrates. Finally, the monolith reactors were calcined at 500 °C for 5 h. The configurations of the monoliths prepared are listed in Table 3.

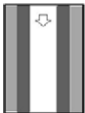
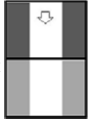
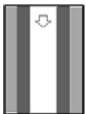
2.3. Reactor system and reaction conditions

The light-off performance of Rh catalysts, both pellet and monolith types, was examined over a fixed-bed continuous flow reactor system by a conventional LOT program, designed to examine the light-off behavior of catalysts for the conversion of reactants [5]. A physical mixture of the catalyst powder (30 wt.%) and the cordierite substrate was pressed, crushed and then screened to obtain catalyst pellet in the 20/30 mesh size for LOT. 0.5 g of the catalyst pellet was mixed with 0.7 cm³ of the glass beads (20/30 mesh size) and then

Table 2
Physical properties of Rh supported on a variety of ZrO₂s.

Catalyst	Rh content (wt.%)		BET surface area (m ² /g)		Active metal area (m ² _{Rh} /g _{catalyst})		Supports
	Fresh	Aged	Fresh	Aged	Fresh	Aged	
Rh/ZrO ₂ (P)	0.16	0.17	42	9	0.457	0.133	ZrO ₂ (precipitation)
Rh/ZrO ₂ (SG)	0.17	0.16	28	<5	0.257	0.106	ZrO ₂ (sol–gel)
Rh/ZrO ₂ (com)	0.18	0.20	10	6	0.178	0.016	ZrO ₂ (commercial)
Rh/ZrO ₂ (P1000)	0.17	0.17	<5	<5	0.161	0.025	ZrO ₂ (ZrO ₂ (P) pre-aged at 1000 °C for 20 h)

Table 3Configuration of monolith reactor system comprised of Rh/ZrO₂ (P) and Pd/Al₂O₃.

Monolith	Powder washcoated ^a	Length of monoliths (in.)	Volume of monoliths (in. ³)	Catalyst components
Double layer 	Top layer: 0.06 wt.% Rh/ZrO ₂ (P)	1	0.3	Rh, Zr
	Bottom layer: 0.35 wt.% Pd/Al ₂ O ₃ Front brick: 0.06 wt.% Rh/ZrO ₂ (P)	1 0.5	0.15	Pd, Al Rh, Zr
Dual brick 	Rear brick: 0.35 wt.% Pd/Al ₂ O ₃ Top layer: 0.06 wt.% Rh catalyst Bottom layer: 0.35 wt.% Pd catalyst	0.5 1 1	0.15 0.3	Pd, Al Rh, Ce, Zr, Al, etc. Pd, Ce, Al, etc.
Commercial 				

^a All three monolith configurations contain equal amounts of NMs.

packed into a 3/8 in. U-type stainless steel tube reactor submerged in a molten-salt bath to ensure an isothermal condition of the catalyst bed during the reaction [20]. The dilution of the catalyst pellet by mixing with the glass beads was to minimize the effect of the exothermic heat generated from TWC reactions and mass transfer limitations in and around the catalyst pellets. The monolithic catalyst bricks (5/8 in. (*D*) × 1 in. (*L*_{total})) wrapped by a ceramic pad were also placed in the 3/4 in. stainless steel tube submerged in the molten salt bath. The temperature difference between the top and bottom of the catalyst bed containing the pellet catalyst (20/30 mesh) was maintained within 4 °C. On the contrary, the monolith reactor system revealed a large temperature difference between the top and bottom of the monolith, reflecting a substantial heat generation by the exothermic TWC reactions over the undiluted monolith reactor system [21].

After the pretreatment of the catalysts at 450 °C under the stoichiometric feed condition ($\lambda = 1.00$), the LOT was conducted over a temperature range from 150 to 450 °C under a slightly lean feed condition ($\lambda = 1.01$) to avoid possible experimental difficulties at the stoichiometric point ($\lambda = 1.00$) [21,22]. Indeed, a catalyst system possessing high deNO_x activity under the lean condition would be more favorable to the design of the aftertreatment system for a fuel efficient automobile including lean-burn engine. The reaction feed stream contained 1% CO, 0.3% H₂, 500 ppm C₃H₆, 500 ppm NO, 1% O₂, 10% CO₂, 10% H₂O and Ar balance. The inlet and outlet gas compositions were monitored by an on-line gas chromatograph (Agilent, Model 6890N) for H₂, O₂, CO and C₃H₆, and by an FT-IR (Thermo Electron Co. Nicolet 5700) for CO, C₃H₆, NO, NH₃ and N₂O. The gas hourly space velocities (GHSV) during the reactions were maintained at 100,000 h⁻¹ and 45,000 h⁻¹ for the pellet and the monolith reactors, respectively.

2.4. Catalyst characterization

The catalyst composition was quantified by inductively coupled plasma-optical emission spectroscopy (ICP-Flame-EOP, Spectro Co.). BET surface areas of the catalysts were calculated from N₂ isotherms obtained at -196 °C by the volumetric method (ASAP2010, Micromeritics Instrument Co.).

The active metallic surface areas (AMSAs) of the catalysts pre-reduced at 450 °C under the 5% H₂/Ar stream were determined by sequential pulse injections of O₂–CO₂–H₂–CO into the catalyst powder at 35 °C (AutoChem II 2920, Micromeritics Instrument Co.) [23]. A H₂ TPR was carried out by the identical chemisorption

apparatus. After the redox treatment of the catalyst at 450 °C, the temperature of the reactor was cooled to 35 °C in Ar flow and then ramped up to 450 °C at 20 °C/min in the 5% H₂/Ar stream at a flow rate of 30 ml/min.

XRD patterns of the catalyst powder were determined by an X-ray diffractometer (PANalytical). The incident X-rays were monochromatized to a wavelength of 1.54056 Å by a Cu K α radiation. XPS spectra of the catalyst samples were also obtained by a VG ESCALAB 220i equipped with an Mg anode. The binding energies of each sample were corrected by the C 1s excited at 284.6 eV.

3. Results and discussion

3.1. Effect of catalyst support on TWC performance of Rh-based catalyst

Rh in TWC has been well known for its important role in removing NO_x in the automotive engine exhaust. However, the Rh supported on Al₂O₃, commonly employed for the TWC system, is prone to catalyst deactivation caused by the high temperature exhaust stream, particularly under an oxidative environment [9]. To prevent and/or mitigate the decrease of the deNO_x performance of the TWC system upon oxidative aging, we examined the effect of catalyst supports, such as Al₂O₃, ZrO₂, CeO₂, C₃Zr₁(Ce_{0.75}Zr_{0.25}O₂), and SiO₂, on the sintering of Rh.

Fig. 1(a) shows the conversion performance of CO, C₃H₆ and NO and the formation of N₂O over the fresh Rh catalysts as a function of the reaction temperature. The Rh/C₃Zr₁ reveals the highest performance for the CO conversion, which may be due to its superior oxygen storage capability improving the catalytic activity for CO oxidation [24,25]. The light-off curves for the CO conversion over Rh/Al₂O₃, Rh/CeO₂ (P) and Rh/ZrO₂ (P) catalysts are varying within 7 °C in terms of *T*₅₀, the temperature where 50% conversion of the reactants is achieved as listed in Table 4, while the Rh/SiO₂ (*T*₅₀ = 246 °C) shows the lowest activity among the catalysts examined. For the C₃H₆ oxidation, the Rh/Al₂O₃ reveals the highest catalytic activity, followed by Rh/ZrO₂ (P), Rh/C₃Zr₁ (CP) and Rh/CeO₂ (CP). They are still in the competitive range of the *T*₅₀. Again, the lowest activity for the C₃H₆ oxidation is observed over the Rh/SiO₂; its *T*₅₀ for the C₃H₆ conversion is not established in the reaction temperature range covered in the present work.

Superior deNO_x performances have been observed over Rh/Al₂O₃ and Rh/ZrO₂ (P) with appreciable amounts of N₂O formation compared to the rest of the catalysts, as shown in Fig. 1(a). Not

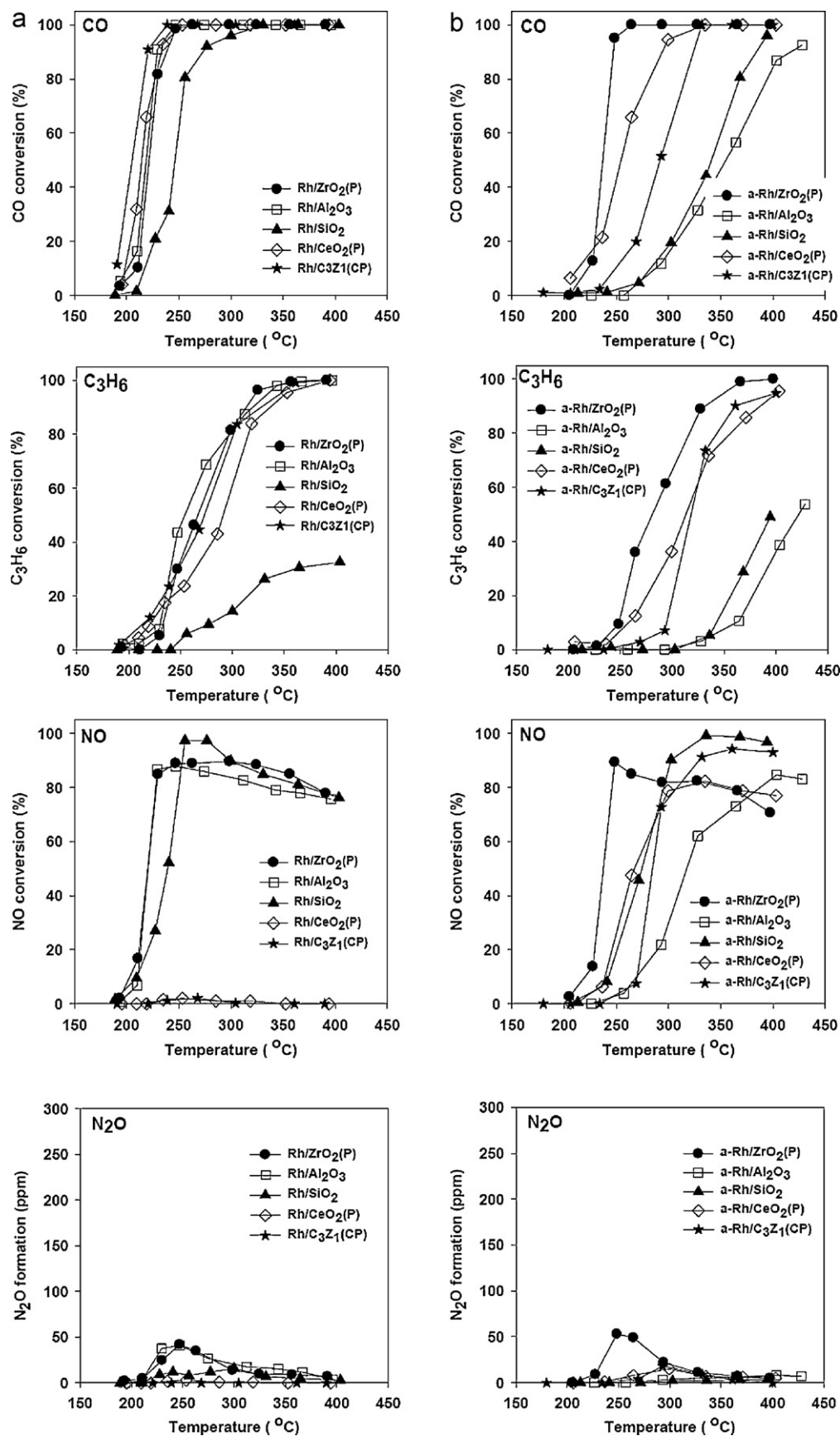


Fig. 1. Light-off curves for CO, C₃H₆ and NO conversion over fresh and aged 0.18 wt.% Rh/metal oxide catalysts during TWC reactions; (a) fresh catalyst, (b) aged catalysts. Reaction feed stream: 1% CO, 0.3% H₂, 500 ppm C₃H₆, 500 ppm NO, 1% O₂, 10% CO₂, 10% H₂O, and Ar balance. GHSV = 100,000 h⁻¹.

Table 4
 T_{50} of fresh and aged Rh/metal oxide catalysts for CO, C₃H₆ and NO conversion.

Catalyst	$T_{50,CO}$ (°C)		T_{50,C_3H_6} (°C)		$T_{50,NO}$ (°C)	
	Fresh	Aged	Fresh	Aged	Fresh	Aged
Rh/Al ₂ O ₃	218	355	254	422	220	317
Rh/SiO ₂	246	341	–	–	239	274
Rh/CeO ₂ (P)	214	254	291	313	–	267
Rh/C ₃ Z ₁ (CP)	205	292	273	319	–	285
Rh/ZrO ₂ (P)	221	237	266	280	219	237

(–): Unable to determine.

unexpected, but still noteworthy, is the fact that the Rh/SiO₂ catalyst, which revealed the lowest oxidation activity for CO and C₃H₆, shows a high NO removal activity. Due to the low oxidation activity of the Rh/SiO₂, the substantial amounts of reductants including H₂, CO and C₃H₆ may be available for the reduction of NO during the course of the reaction. In particular, the superior NO conversion activity of the a-Rh/SiO₂ compared to that of the a-Rh/ZrO₂ (P) at high temperature above 250 °C may be due to the NO + H₂ reaction to produce NH₃ at 250–350 °C, followed by the NO + CO reaction above 350 °C over the a-Rh/SiO₂, while the a-Rh/ZrO₂ (P) starts to suffer from shortage of effective reductants such as CO above its light-off temperature for NO conversion. In addition, NO is hardly reduced over Rh/CeO₂ (P) and Rh/C₃Z₁ (CP) under the slightly lean condition ($\lambda = 1.01$) employed, over the entire temperature range. The dominant oxidation activity of the Rh ceria based catalysts toward CO and C₃H₆ is probably the major cause for the poor NO removal performance, resulting from the shortage of the reductants [10,26]. Overall, ZrO₂ (P) and Al₂O₃ seem to be suitable supports for Rh to simultaneously remove CO, C₃H₆ and NO over the fresh TWC system.

On the contrary, catalyst deactivation is observed over the Rh catalysts upon thermal aging at 1000 °C for 20 h in the static air. As shown in Fig. 1(b), the a-Rh/ZrO₂ (P) reveals the highest TWC performance and a superior thermal durability among the catalysts examined for all three reactions. The shifts of the light-off curves for CO, C₃H₆ and NO conversions to the higher temperature region are clearly observed over the a-Rh/SiO₂ and a-Rh/Al₂O₃. Interestingly, the a-Rh/CeO₂ (P) and a-Rh/C₃Z₁ (CP) show the NO conversions, which were hardly observed over their fresh counterparts. Haneda et al. [10] reported similar results of the increased NO conversion over the aged Rh ceria based catalysts. They speculated that the Rh species on CZ support for the NO reduction may be stabilized by thermal aging.

The causes of the catalyst deactivation include the simple sintering of Rh, the encapsulation of Rh by pore blocking of the support and/or the inactivation of Rh species by the formation of a Rh-support complex upon aging [27,28]. As listed in Table 1, the BET surface areas of all catalysts decrease upon thermal aging. The alteration of the AMSAs of the Rh catalysts is directly related to their thermal durability. The a-Rh/Al₂O₃ lost about 95% of its active metal surface area upon aging as listed in Table 1. There was no loss of Rh content upon the thermal aging, suggesting that thermal deactivation is due to the decreased number of the exposed active Rh sites on the catalyst surface, due either to the formation of the Rh aluminate or to the encapsulation of Rh by the support. Yao et al. [9,29] reported that Rh can diffuse into Al₂O₃ to form Rh aluminate during the thermal sintering, resulting in the decrease of the redox capability of the active Rh sites.

Indeed, the a-Rh/Al₂O₃ reveals no H₂ consumption peak during the catalyst reduction up to 300 °C during the TPR as depicted in Fig. 2, while the fresh one clearly shows the broad reduction peaks to be assigned to the reduction of Rh₂O₃ (130 °C), RhO_x (200 °C) and Rh-alumina interaction (270 °C), respectively [30]. Similar to the a-Rh/Al₂O₃ catalyst, the a-Rh/SiO₂ with the low

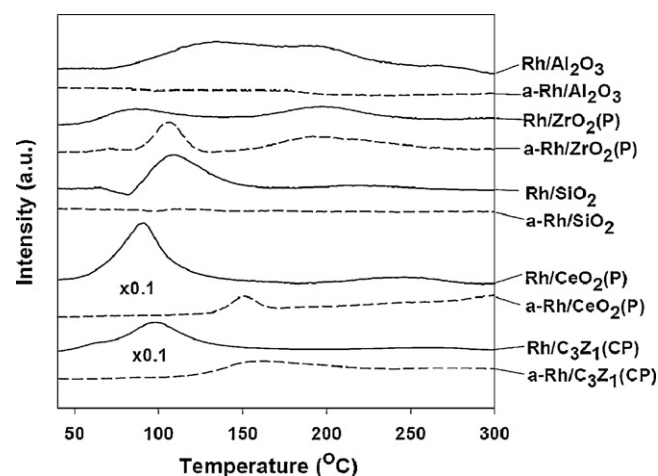


Fig. 2. TPR profiles over fresh (solid line) and aged (dash line) Rh/metal oxide catalysts. The intensities of TPR profiles over the fresh and aged ceria based catalysts including Rh/CeO₂ and Rh/C₃Z₁ are reduced by 10 times (denoted as "×0.1").

AMSA (0.013 m²_{Rh}/g_{catalyst}) reveals no H₂ consumption peak for the reduction of the Rh oxides up to 300 °C as shown in Fig. 2, although a single peak for the reduction of Rh₂O₃ over the fresh one is observed at 110 °C. Thus, the significant decrease of the TWC performance over the a-Rh/SiO₂ is believed to be due mainly to the formation of inactive Rh compounds, probably Rh silicide [31].

On the contrary, a-Rh/CeO₂ (P) and a-Rh/C₃Z₁ (CP) reveal a moderate catalyst deactivation due to their larger AMSAs remaining than that of the a-Rh/Al₂O₃ and a-Rh/SiO₂, as listed in Table 1. As shown in Fig. 2, the fresh Rh/CeO₂ reveals a strong H₂ consumption peak at around 90 °C to be assigned to the reduction of Rh₂O₃ and Rh-ceria interface [32]. In addition, a broad peak by the reduction of the surface cerium compound has been observed at around 250 °C [5]. The Rh/C₃Z₁ catalyst displays a reduction trend similar to that of the Rh/CeO₂. The areas of the H₂ consumption peaks over both Rh/CeO₂ and Rh/C₃Z₁ are nearly 10 times larger than those over the rest of the Rh/metal oxide catalysts, probably due to the strong H₂ spill-over from Rh to the support over the ceria-based catalysts at this temperature [33]. Note that the intensities of H₂ consumption peaks for Rh/CeO₂ and Rh/C₃Z₁ have been reduced by 1/10 time as noted in Fig. 2.

Unlike a-Rh/Al₂O₃ and a-Rh/SiO₂, the H₂ consumption peaks by the reductions of Rh₂O₃ and surface ceria over both ceria-based catalysts shift to higher temperatures with decreased peak intensities upon aging. An apparent reduction peak has been observed at 150 °C over a-Rh/CeO₂, while a-Rh/C₃Z₁ shows a broad peak with the maximum H₂ consumption at 160 °C. Although no change of the amount of Rh included in the catalysts is observed upon aging as listed in Table 1, both aged ceria-based catalysts do not exhibit the reduction peaks of surface Rh₂O₃, reportedly observed at 130 °C during the TPR [34]. The primary deactivation cause for the ceria-based Rh catalysts upon aging may then be the loss of the active Rh species from the surface of the CeO₂ or C₃Z₁ supports due to the diffusion of Rh into the supports [35], unlike the formation of the inactive Rh species in the form of Rh aluminate and Rh silicide upon the aging of Rh/Al₂O₃ and Rh/SiO₂, respectively [9,29,31].

The Rh/ZrO₂ (P), revealing the strongest thermal durability among the catalysts examined in the present study, maintains the highest AMSA even after aging. Moreover, the apparent reduction of the surface Rh oxides over the a-Rh/ZrO₂ (P) has been also observed during the TPR as shown in Fig. 2. The deactivation cause for the Rh/ZrO₂ will be further discussed in Section 3.3.

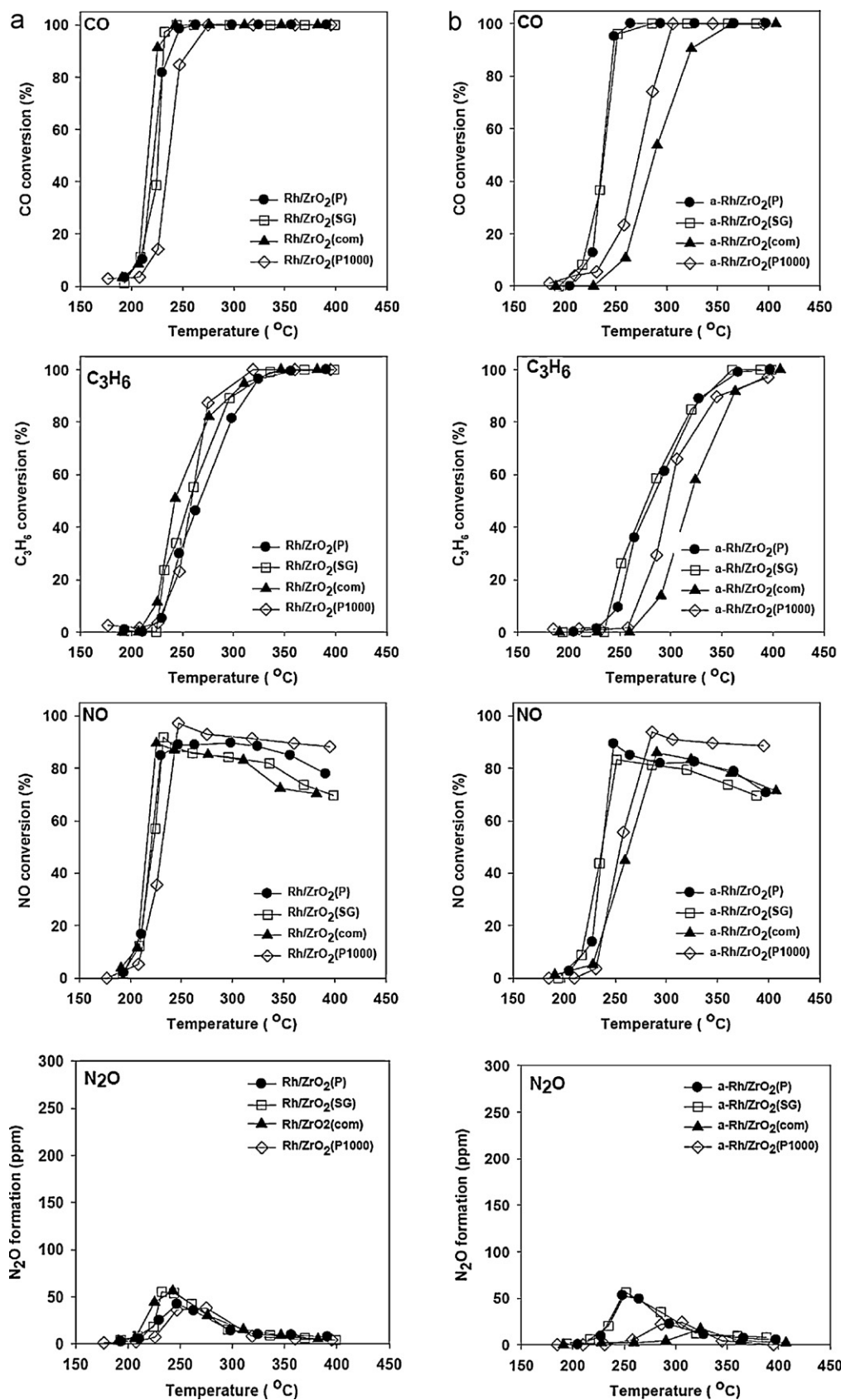


Fig. 3. Light-off curves for CO, C₃H₆ and NO conversion over fresh and aged Rh/ZrO₂ catalysts during TWC reactions; (a) fresh and (b) aged Rh/ZrO₂ catalysts. Reaction feed stream: 1% CO, 0.3% H₂, 500 ppm C₃H₆, 500 ppm NO, 1% O₂, 10% CO₂, 10% H₂O, and Ar balance. GHSV = 100,000 h⁻¹.

3.2. Effect of ZrO₂ prepared by a variety of methods on TWC performance

Since Rh/ZrO₂ (P) has shown superior TWC activities for the removal of CO, C₃H₆ and NO after aging, the ZrO₂ supports prepared by a variety of methods have been examined to further improve the activity and thermal durability of the Rh/ZrO₂ TWC system. Indeed, the physicochemical property of ZrO₂ is dependent on its preparation methods and procedures [14,16]. Two types of ZrO₂ supports were prepared by the precipitation and sol–gel methods followed by calcination at 700 °C for 5 h in static air. The ZrO₂ (P) support prepared was further calcined at 1000 °C for 20 h in static air, an additional calcination step which was identical to the thermal aging condition employed in the present study. This ZrO₂ (P) thermally pre-aged with the extra calcination was denoted by ZrO₂ (P1000). To compare the activities of the Rh/ZrO₂ catalysts prepared, the Rh supported on a commercial ZrO₂ (Hanawa) was also prepared. Their physicochemical properties before and after aging are listed in Table 2.

As shown in Fig. 3(a), both Rh/ZrO₂ (SG) and (com) catalysts exhibit similar light-off curves to the fresh Rh/ZrO₂ (P) for all three reactions. Negligible shifts of the light-off curves within the narrow temperature range are observed over all of the fresh ZrO₂-supported Rh catalysts. When the catalysts are aged at 1000 °C for 20 h in static air, the degree of the catalyst deactivation depends on the ZrO₂ supports employed as depicted in Fig. 3(b).

Two distinct catalyst deactivation trends, however, are apparent over the a-Rh/ZrO₂ catalysts. As summarized in Table 5, the shifts of T₅₀s for CO, C₃H₆ and NO conversions over the a-Rh/ZrO₂ (P) and a-Rh/ZrO₂ (SG) are within 20 °C. However, severe deactivations of the Rh/ZrO₂ (com) and Rh/ZrO₂ (P1000) have been observed. The upward shifts of the T₅₀s for CO, C₃H₆ and NO conversions ranging from 25 to 76 °C over both Rh/ZrO₂ (com) and Rh/ZrO₂ (P1000) upon aging are much higher than those over the Rh/ZrO₂ (P) and Rh/ZrO₂ (SG) as listed in Table 5. Note that the alteration of T₅₀ also varies with respect to the TWC reactions. The results indicate that the thermal durability of the Rh/ZrO₂ strongly depends on the physicochemical properties of ZrO₂ supports, which in turn depend on their preparation methods. It is worth nothing that the purity of ZrO₂ prepared by the SG and P methods in the present study may be higher than that of the commercial ZrO₂.

3.3. Deactivation of Rh/ZrO₂ catalysts by oxidative thermal aging

3.3.1. Physicochemical properties of Rh/ZrO₂ catalysts

As listed in Table 2, both BET and active metal surface areas of the Rh/ZrO₂ catalysts decreased upon aging. The decrease of the TWC performance of the Rh/ZrO₂ catalysts upon aging may be understood by the alteration of their AMSAs. Nearly 90% of the AMSAs of the Rh/ZrO₂ (P1000 and com) catalysts disappeared upon aging; however, 29–41% of the AMSAs of the Rh/ZrO₂s (P and SG) still remained. They maintain more than 4 or 8 times higher AMSAs of Rh than the a-Rh/ZrO₂s (P1000 and com). The loss of AMSA of the Rh species on the catalyst surface upon aging may then elucidate the deactivation trend of the Rh/ZrO₂s (P and SG) compared to the trend of Rh/ZrO₂s (P1000 and com) catalysts. For all catalyst listed

Table 5

T₅₀ of fresh and aged Rh/ZrO₂ catalysts for CO, C₃H₆ and NO conversion.

Catalyst	T _{50,CO} (°C)		T _{50,C₃H₆} (°C)		T _{50,NO} (°C)	
	Fresh	Aged	Fresh	Aged	Fresh	Aged
Rh/ZrO ₂ (P)	221	237	266	280	219	237
Rh/ZrO ₂ (SG)	226	237	256	276	222	237
Rh/ZrO ₂ (com)	216	287	241	317	215	264
Rh/ZrO ₂ (P1000)	236	272	259	297	230	255

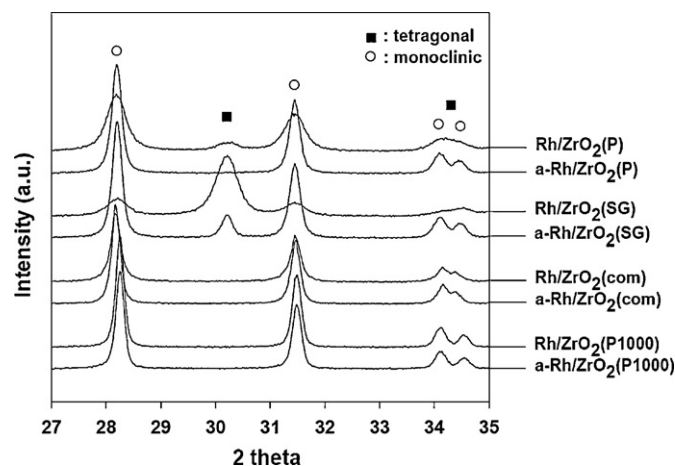


Fig. 4. XRD patterns over fresh and aged Rh/ZrO₂ catalysts; (○) monoclinic and (■) tetragonal phase.

in Table 2, no loss of Rh content in the Rh/ZrO₂ catalysts before and after aging has been observed by the ICP-OES analysis. The primary cause of deactivation of the Rh/ZrO₂ catalysts may then be the loss of the number of the active Rh sites on the surface of the catalyst supports upon aging.

The phase of ZrO₂ supports prepared has been examined to explain the strong thermal stability of the Rh/ZrO₂ (P and SG) catalysts. Monoclinic and tetragonal phases have been widely recognized as the primary state of ZrO₂, which are reversibly transformed during thermal treatment [36]. From XRD patterns over the fresh Rh/ZrO₂ catalysts as shown in Fig. 4, the Rh/ZrO₂ (P and SG) catalysts have both tetragonal and monoclinic phases as marked by (■) and (○), respectively. However, only the monoclinic phase exists over the Rh/ZrO₂ (P1000 and com) catalysts. It is not surprising that the phase of ZrO₂ in the Rh/ZrO₂ (P1000) is monoclinic, mainly due to the pre-aging of ZrO₂ (P) at 1000 °C for 20 h prior to the impregnation of Rh [36,37].

Upon aging, the transformation of the tetragonal phase of ZrO₂ in the Rh/ZrO₂ (P) to the monoclinic phase appears complete (Fig. 4), even though the exact extent of this transformation cannot be determined by the XRD due to the limitation of the XRD analysis. On the contrary, the tetragonal phase of ZrO₂ still remains in the a-Rh/ZrO₂ (SG) after its partial transformation to the monoclinic phase. No further change of phases over the Rh/ZrO₂ (P1000 and com) catalysts has been observed after the thermal aging. Noting that the thermal deactivation of the Rh/ZrO₂ (P and SG) catalysts was less severe than that of the Rh/ZrO₂ (P1000 and com) catalysts (Fig. 3), we conclude that the tetragonal phase of ZrO₂ for the support of Rh likely plays an important role for preventing the deactivation of Rh species by thermal aging under the realistic oxidative exhaust conditions of the gasoline engine [7].

3.3.2. Rh state on ZrO₂ supports

The states of Rh species on the surface of the ZrO₂ supports including the tetragonal and monoclinic phases have been examined by XPS to determine the alteration of the state of Rh on a variety of the ZrO₂ supports upon aging. Fig. 5 shows the XPS spectra obtained over the fresh and aged Rh/ZrO₂ catalysts. A major peak to be assigned to Rh³⁺ was observed over the fresh Rh/ZrO₂ catalysts in the range of the XPS binding energy from 308.1 to 308.6 eV for all ZrO₂ supports examined [12,38]. Neither a shift in the binding energy nor a change of the intensity of XPS spectra for Rh³⁺ was observed over the Rh/ZrO₂s (P and SG) upon aging, reflecting no disappearance of Rh³⁺ species from the catalyst surface of the Rh/ZrO₂s (SG and P) containing both monoclinic and tetragonal phases.

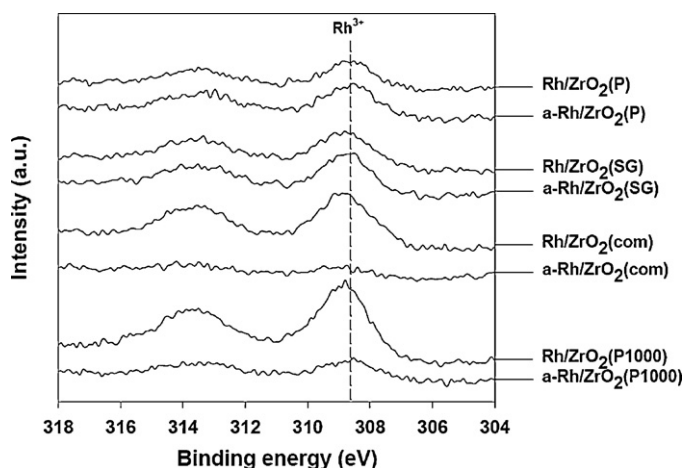


Fig. 5. XPS spectra (Rh 3d) of fresh and aged Rh/ZrO₂ catalysts.

However, a significant amount of the surface Rh³⁺ disappeared over the a-Rh/ZrO₂s (P1000 and com) containing only the monoclinic ZrO₂ as evidenced by their XPS peak intensities. A small amount of Rh³⁺ still remains over the a-Rh/ZrO₂ (P1000) after aging, but no Rh³⁺ XPS peak can be observed over the a-Rh/ZrO₂ (com). This observation may well explain the relative decrease of the AMSAs of the a-Rh/ZrO₂s (P1000 and com). The severe thermal deactivation of the Rh/ZrO₂s (P1000 and com) as shown in Fig. 3 can now be understood by the disappearance of Rh³⁺ from the surface of the catalyst.

Similar to the diffusion of Pt on the catalyst surface into a sublattice region of the support by thermal treatment of Pt/CeO₂–ZrO₂–La₂O₃ at 900 °C for 3 h as reported by Fan et al. [35], Rh may diffuse into the sublattice of the monoclinic ZrO₂ supports during aging, while the tetragonal phase in the ZrO₂s (SG and P) prevents the diffusion of Rh into the sublattice region of ZrO₂ due to the Rh-tetragonal interaction [39,40]. Since the BET surface areas of the ZrO₂s (P1000 and com) containing the monoclinic phase are extremely low, the burial mechanism of Pt by Fan et al. [35] may also be applicable to the aging trend of the Rh/ZrO₂ catalysts examined in this study. Note that the tetragonal phase ZrO₂ in the fresh Rh/ZrO₂s (SG and P) plays an important role in moderating the disappearance of Rh species from the ZrO₂ surface upon aging. Although the tetragonal phase ZrO₂ in a-Rh/ZrO₂ (P) is not observed by XRD, it can be stabilized by Rh in the temperature region higher than 900 °C, implying that a small fraction of the tetragonal phase may remain upon aging in the a-Rh/ZrO₂ (P) to interact with Rh [40].

3.3.3. Redox properties of Rh/ZrO₂ catalysts

Fig. 6 shows the H₂ TPR profiles for the fresh and aged Rh/ZrO₂ catalysts. For the Rh/ZrO₂ (P and SG) catalysts, two major reduction peaks can be observed in the temperature range below 130 °C and at around 200 °C. The Rh/ZrO₂ (P1000 and com) catalysts containing the monoclinic ZrO₂ reveal a H₂ consumption peak up to 130 °C during TPR without any high temperature peak in the temperature range up to 300 °C. Fornasiero et al. [34] reported that the reduction peaks at around 80 and 110 °C arise from the reduction of well-dispersed surface Rh₂O₃ and bulk-like large crystalline of surface Rh₂O₃, respectively. Zhang et al. [39,40] suggested that the peak at around 200 °C is due to the reduction of Rh³⁺ stabilized on the tetragonal phase of ZrO₂, indicating the interaction of Rh³⁺ with tetragonal ZrO₂. Listed in Table 6 are the amounts of H₂ consumed by the reduction of the surface Rh oxides, the sublattice Rh oxides and the Rh that interacted with tetragonal ZrO₂ during TPR.

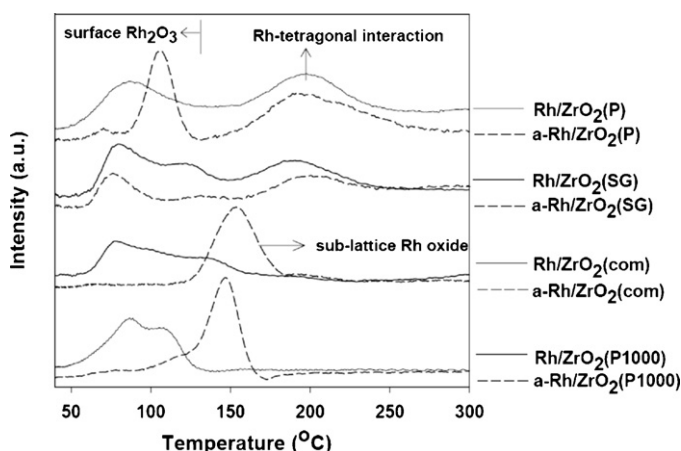


Fig. 6. TPR profiles over fresh (solid line) and aged (dash line) Rh/ZrO₂ catalysts.

The shifts and/or the decrease of intensities of the H₂ TPR peaks are evident over the a-Rh/ZrO₂ catalysts upon aging. The a-Rh/ZrO₂ (P) reveals a small shoulder peak at around 70 °C and a strong reduction peak at 110 °C due to the reduction of the large Rh₂O₃ particles formed by sintering of Rh metal [9,34]. Although the a-Rh/ZrO₂ (SG) still exhibits the reduction of the well-dispersed Rh₂O₃ at around 80 °C with a small shoulder at around 130 °C, the sintering of Rh on this catalyst is indicated by the decrease of the peak intensities and the AMSA as listed in Table 2. Indeed, the remaining portions of AMSA of the Rh/ZrO₂ (P and SG) are 29 and 41% after aging, as listed in Table 2, an indication of a faster sintering rate of Rh oxide particles on the surface of the a-Rh/ZrO₂ (P) than those on the a-Rh/ZrO₂ (SG) surface. Interestingly, these two aged catalysts still keep the reduction peak at around 200 °C assigned to the interaction of Rh³⁺ with the tetragonal-like ZrO₂ phase, although the tetragonal phase of ZrO₂ was not observed in the a-Rh/ZrO₂ (P) by XRD in Fig. 4 [39,40]. As listed in Table 6, there is no effect of aging on the H₂ consumption for the reduction of the Rh-tetragonal ZrO₂ in both catalysts. This observation may imply that the interaction of Rh³⁺ with the tetragonal ZrO₂ is strong enough to withstand the aging condition, preventing Rh from diffusing into the sublattice of ZrO₂ to cause the burial of Rh. Given the similar deactivation behavior exhibited by both catalysts, such as the decrease of the AMSAs of Rh species, the Rh-tetragonal ZrO₂ interaction evidenced by TPR and the presence of Rh on the surface of the catalysts determined by XPS, the primary cause for the deactivation upon the thermal aging of the Rh/ZrO₂ (SG and P) catalysts appears most likely to be the sintering of Rh [9,34].

On the contrary, the a-Rh/ZrO₂ (com) shows only one reduction peak centered at 150 °C with no H₂ consumption by the reduction of the surface Rh oxides below 130 °C, while the a-Rh/ZrO₂ (P1000) reveals a strong reduction peak at around 145 °C with a small shoulder peak at 110 °C. No reduction peak by the interaction of Rh with the tetragonal ZrO₂ has been observed over both a-Rh/ZrO₂ (P1000 and com) catalysts. Since the reduction of the surface Rh₂O₃ is typically completed around 130 °C and the Rh oxides interacting with the tetragonal ZrO₂ start to be reduced from 200 °C [34,39,40], the intense reduction peak at around 150 °C of the a-Rh/ZrO₂ (com and P1000) may be assigned to the reduction of the sublattice Rh oxides in the monoclinic ZrO₂ phase formed by the burial mechanism. Indeed, the Rh species were only barely detectable on the surface of the a-Rh/ZrO₂s (P1000 and com) as determined by XPS (Fig. 5), even though the Rh content remained unchanged upon the thermal aging as determined by ICP-OES (Table 2). In addition, it has been reported that no restoration of Rh over the aged Rh/ZrO₂ is achieved even by the reductive treatment with H₂ [9], indicating

Table 6
H₂ consumption over Rh/ZrO₂ catalysts during TPR.

Catalyst	Surface Rh oxides ($\mu\text{mol}_{\text{H}_2}/\text{g}_{\text{catalyst}}$)		Sublattice Rh oxides ($\mu\text{mol}_{\text{H}_2}/\text{g}_{\text{catalyst}}$)		Rh-tetragonal interaction ($\mu\text{mol}_{\text{H}_2}/\text{g}_{\text{catalyst}}$)	
	Fresh	Aged	Fresh	Aged	Fresh	Aged
Rh/ZrO ₂ (P)	15.4	16.6	–	–	16.5	17.1
Rh/ZrO ₂ (SG)	16.9	10.0	–	–	9.5	9.3
Rh/ZrO ₂ (com)	20.8	–	–	20.0	–	–
Rh/ZrO ₂ (P1000)	23.7	3.9	–	20.5	–	–

(–): Unable to determine.

that the buried Rh may hardly diffuse out of the sublattice region of ZrO₂ to the surface of the catalyst.

As listed in Table 6, the amounts of H₂ consumed by the sublattice Rh oxides over the a-Rh/ZrO₂ (com and P1000) are quite similar to those by the surface Rh oxides over their fresh counterparts. It indicates that the surface Rh oxides are mainly transformed into the sublattice Rh oxides on the monoclinic ZrO₂ by the oxidative thermal aging employed. Particularly, the small shoulder consuming $3.9 \mu\text{mol}_{\text{H}_2}/\text{g}_{\text{catalyst}}$ at 110 °C during the TPR observed over the a-Rh/ZrO₂ (P1000) indicates that the a-Rh/ZrO₂ (P1000) still holds a small amount of the surface Rh₂O₃ that is absent on the surface of the a-Rh/ZrO₂ (com), as determined by the amounts of H₂ consumption listed in Table 6. The slightly stronger thermal stability of the a-Rh/ZrO₂ (P1000) than that of the a-Rh/ZrO₂ (com) may now be understood.

Since the monoclinic and tetragonal ZrO₂s are stable and metastable, respectively, due to the different zirconium coordination numbers [41,42], a stronger interaction of Rh with the tetragonal ZrO₂ may be anticipated than that with the monoclinic ZrO₂. Indeed, the coordination numbers of Zr over the monoclinic and tetragonal ZrO₂s are seven and eight, respectively [42]. Zhang et al. [39,40] also reported the strong interaction of Rh with the tetragonal ZrO₂ in a TPR study. A similar interaction of Pt with the tetragonal ZrO₂ has also been observed [43].

3.3.4. Deactivation mechanism of Rh/ZrO₂ catalysts

As illustrated in Fig. 7, Rh can be dispersed on ZrO₂ support in a form of small Rh₂O₃ particles before aging, regardless of the phase of ZrO₂, monoclinic and/or tetragonal. In particular, Rh strongly interacts with the tetragonal phase of ZrO₂, whereas it hardly does so with the monoclinic phase of ZrO₂. Upon aging, the Rh₂O₃ particles on the tetragonal phase become larger by agglomeration, while the Rh₂O₃ supported on the monoclinic phase is sintered and

diffused into the sublattice region of the support according to the burial mechanism proposed.

However, the strong Rh-tetragonal ZrO₂ interaction over the Rh/ZrO₂s (SG and P) may prevent the burial of Rh into the sublattice region of ZrO₂. In addition, the sublattice Rh oxides located in monoclinic ZrO₂ may not be readily reduced and/or oxidized compared to the surface Rh₂O₃, but the apparent loss of TWC performance and the redox property of the catalyst has been observed as clearly shown in Figs. 3 and 4. The more severe deactivation of the a-Rh/ZrO₂ (P1000 and com) catalysts by thermal aging compared to that of the a-Rh/ZrO₂s (SG and P) is now understood by the burial mechanism of Rh into the sublattice region of ZrO₂ specific for the Rh supported on the monoclinic ZrO₂.

3.4. Application of Rh/ZrO₂ to commercial TWC converter

3.4.1. Formation of NH₃ over Rh/metal oxide catalysts during TWC reaction

Since the Rh catalyst in the front monolith brick of the TWC converter can produce NH₃ during the NO_x reduction, the overall NO_x conversion can be decreased by the reoxidation of this NH₃ to NO_x over the oxidation catalysts in the rear part of the converter [6]. Thus, the Rh catalyst for the NO_x reduction should be thermally stable, but should not produce too much NH₃ when combined with an oxidation catalyst such as Pd/Al₂O₃. For this reason, the formation of NH₃ has been examined over Rh/metal oxide catalysts during the TWC reaction.

Fig. 8(a) shows the amount of NH₃ formed over the fresh Rh/metal oxide catalysts during the TWC reaction under a simulated gasoline engine exhaust condition as a function of reaction temperature. At 230 °C, the fresh Rh/Al₂O₃ and Rh/ZrO₂ (P) produce a large amount of NH₃, 180 and 157 ppm, respectively. The highest amount of NH₃ is formed over the fresh Rh/SiO₂ in a wide range of

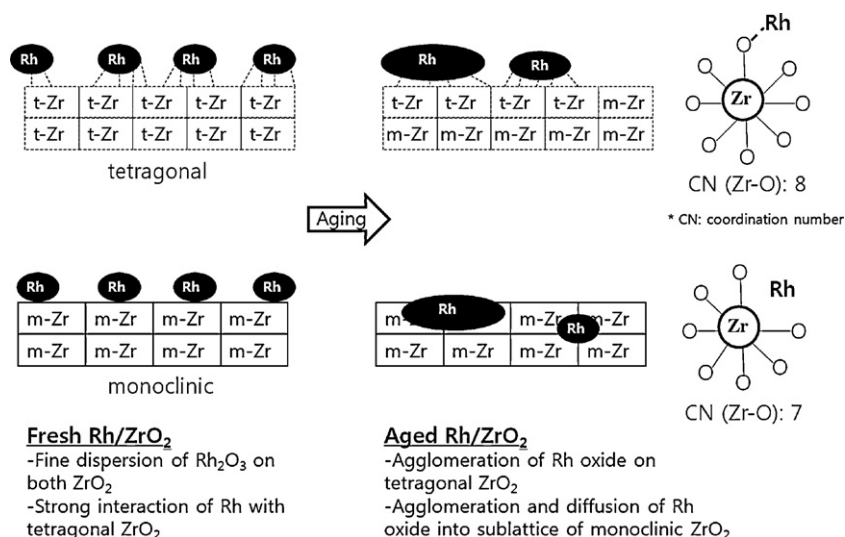


Fig. 7. Schematic deactivation process of Rh/ZrO₂ catalysts.

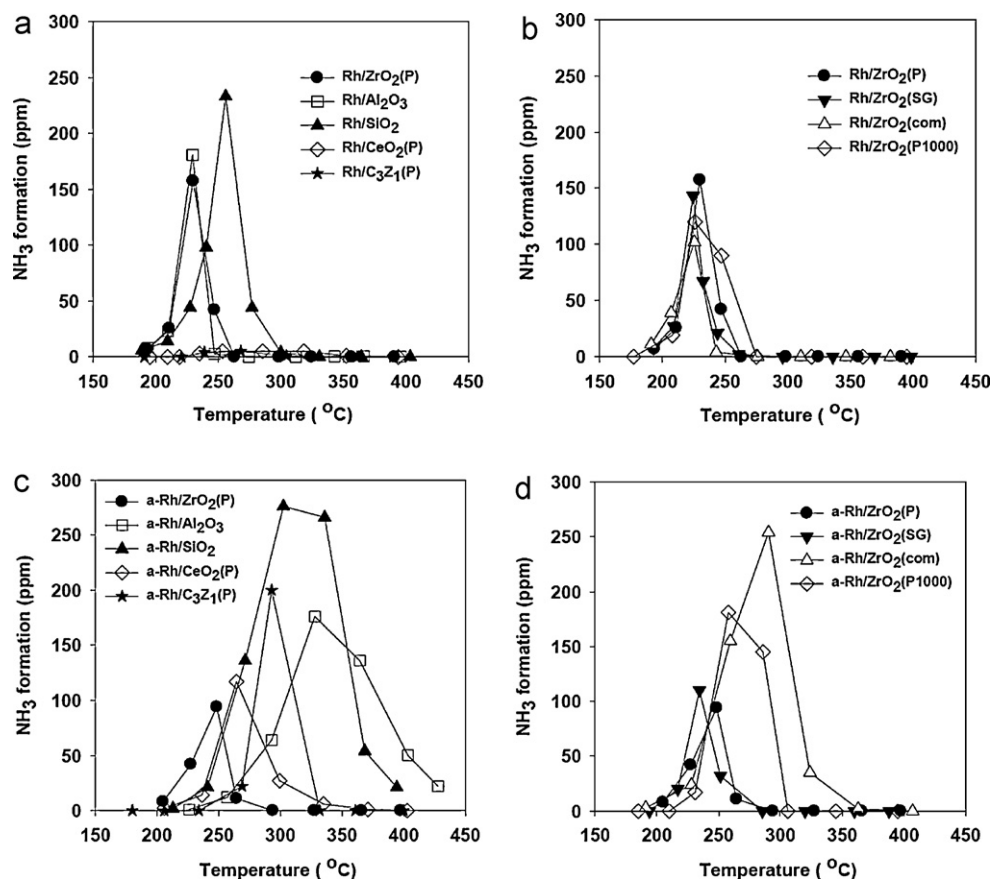


Fig. 8. NH_3 formation over Rh catalysts; fresh (a) Rh/metal oxides and (b) Rh/ ZrO_2 catalysts; aged (c) Rh/metal oxides and (d) Rh/ ZrO_2 catalysts. Reaction feed stream: 1% CO, 0.3% H_2 , 500 ppm C_3H_6 , 500 ppm NO, 1% O_2 , 10% CO_2 , 10% H_2O , and Ar balance. GHSV = 100,000 h^{-1} .

the reaction temperature from 200 to 300 °C. The maximum concentration of NH_3 during the reaction reaches 233 ppm at 256 °C. The formation of NH_3 is closely related to the NO reduction activity over the Rh-based catalysts, as shown in Fig. 1(a). The high NO reduction activity of the Rh/ SiO_2 is mainly due to the formation of NH_3 during the course of the NO reduction reaction. Negligible amounts of NH_3 are formed over the Rh/ CeO_2 and C_3Z_1 , which is in line with the poor de NO_x activity of the fresh ceria-based Rh catalysts, as shown in Fig. 1(a). As shown in Fig. 8(b), Rh supported on a variety of ZrO_2 also produces a significant amount of NH_3 at around 230 °C during the course of the TWC reaction.

Drastic changes have been observed in the maximum amount and the temperature window of the NH_3 formation over the Rh/metal oxide and Rh/ ZrO_2 catalysts upon aging, as shown in Fig. 8(c) and (d). The a-Rh/ Al_2O_3 produces a substantial amount of NH_3 above 290 °C and the concentration of NH_3 produced reaches 176 ppm at 328 °C. Since NH_3 can be readily oxidized to N_2 and/or NO_x over Pd/ Al_2O_3 simultaneously employed along with Rh-based catalyst over the TWC system [44], the a-Rh/ Al_2O_3 may not be a promising candidate as a de NO_x catalyst in view of its NH_3 formation. As depicted in Fig. 8(d), the a-Rh/ ZrO_2 (P and SG) catalysts produce the 94 and 110 ppm of NH_3 at 235 and 249 °C within the narrow temperature range, respectively. Among the catalysts examined in the present study, the Rh/ ZrO_2 (P and SG) catalysts have shown the strongest thermal durability. Both facts consistently reflect the promise of ZrO_2 as a support for Rh for the TWC system.

The a-Rh/ ZrO_2 (com and P1000) catalysts also produce a substantial amount of NH_3 . 254 and 181 ppm of NH_3 are formed over the a-Rh/ ZrO_2 (com and P1000) at 290 and 258 °C, respectively. Up to 50% of NO in the feed gas stream is converted to NH_3 over

the a-Rh/ ZrO_2 (com and P1000) catalysts. Upon thermal aging, the amount of NH_3 produced over the Rh/ ZrO_2 s (com and P1000) increases dramatically. The aged ceria-based catalysts (a-Rh/ CeO_2 and C_3Z_1) also produce a significant amount of NH_3 between 200 and 350 °C, although they hardly produce NH_3 before aging. Particularly, the a-Rh/ C_3Z_1 produces 200 ppm of NH_3 at 293 °C.

Although the a-Rh/ SiO_2 catalyst reveals a superior NO conversion performance above 300 °C even under the slightly lean condition (Fig. 1(b)), it produces the largest amount of NH_3 (276 ppm at 303 °C) in a wide range of the reaction temperature up to 350 °C among the catalysts examined (Fig. 8(c)). Indeed, 210 ppm of H_2 reacted to produce the nearly stoichiometric amount of NH_3 (136 ppm) through the NO + H_2 reaction at 270 °C, where no O_2 consumption was observed. More than 50% of NO in the feed stream is converted to NH_3 over the a-Rh/ SiO_2 from 300 to 350 °C during the course of the TWC reaction. It implies that the Rh/ SiO_2 is not a preferable de NO_x catalyst for the TWC system, but the a-Rh/ SiO_2 catalyst may be a useful catalytic formulation for the passive NH_3 /SCR system recently proposed [45]. The Rh catalyst for NO_x reduction is commonly combined with oxidation catalysts such as Pd or Pt, in order to complement its relatively low oxidation activities for CO and HCs. Since the Rh/ ZrO_2 s (P and SG) have shown the strongest thermal stability with the moderate production of NH_3 , the Rh/ ZrO_2 is a promising catalyst for improving catalytic activity and thermal durability of an advanced TWC system.

3.4.2. Monolith configuration of Pd/ Al_2O_3 -Rh/ ZrO_2 bimetal TWC

The feasibility of Rh/ ZrO_2 as a primary catalyst component for removing NO_x over the TWC system has been investigated using a monolith catalyst washcoated with the powders of Rh/ ZrO_2 (P) and

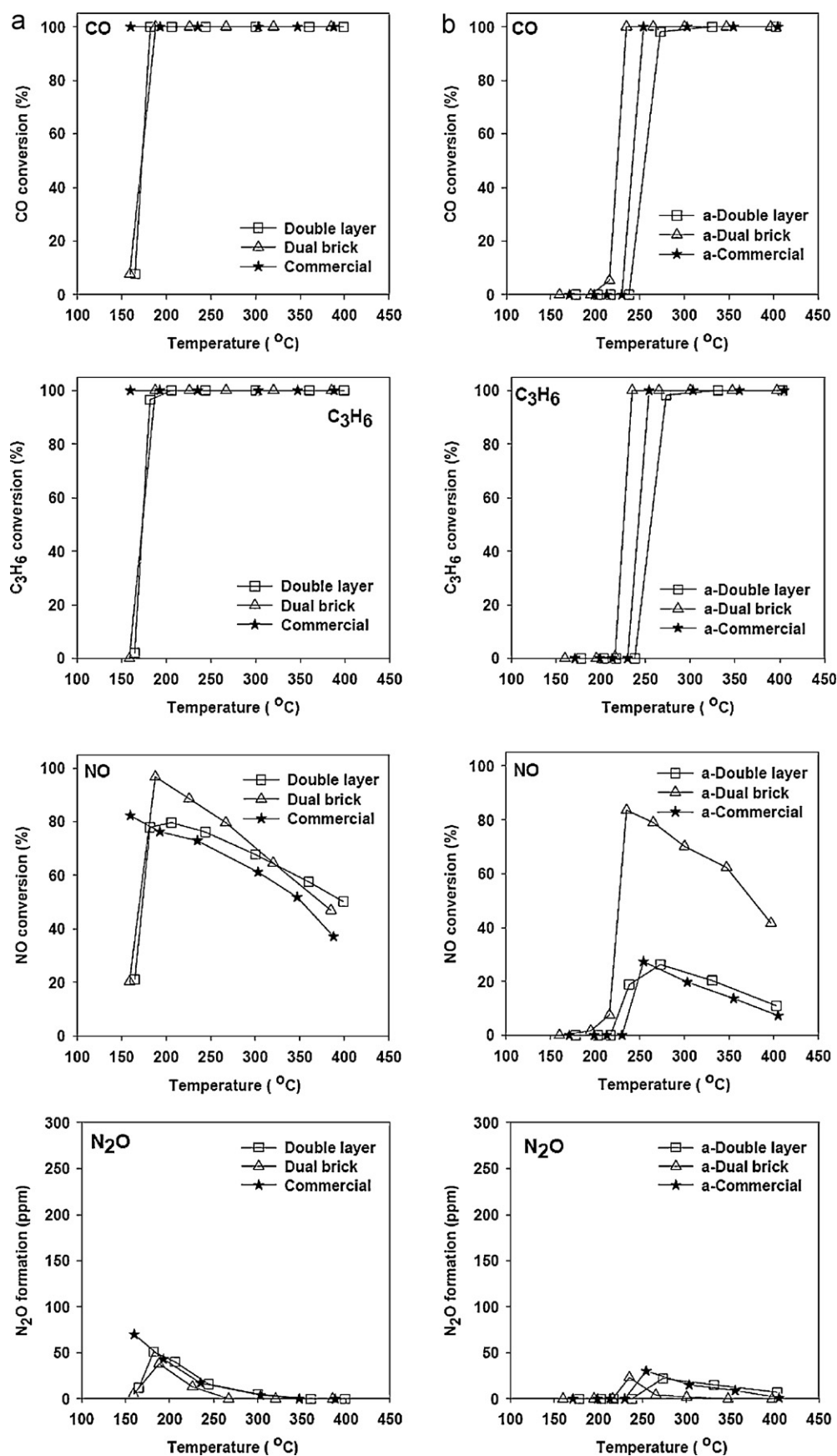


Fig. 9. Light-off curves for CO, C₃H₆ and NO conversion over fresh and aged monolithic catalysts during TWC reactions; (a) fresh and (b) aged monoliths. Reaction feed stream: 1% CO, 0.3% H₂, 500 ppm C₃H₆, 500 ppm NO, 1% O₂, 10% CO₂, 10% H₂O, and Ar balance. GHSV = 45,000 h⁻¹.

Table 7
 T_{50} of fresh and aged monoliths for CO, C₃H₆ and NO conversion.

Catalyst	$T_{50,CO}$ (°C)		T_{50,C_3H_6} (°C)		$T_{50,NO}$ (°C)	
	Fresh	Aged	Fresh	Aged	Fresh	Aged
Commercial	<150	242	<150	242	<150	–
Double layer	172	261	173	261	174	–
Dual brick	172	225	174	225	170	227

(–): Unable to determine.

the Pd/ γ -Al₂O₃ catalysts. A commercial TWC monolith fabricated in the form of a double-layer has been also employed for a comparative kinetic study. Double-layered and dual-brick monoliths were prepared in order to examine the TWC activities and thermal stabilities of the monolith reactors with respect to the configuration of the Rh/ZrO₂ (P) and Pd/Al₂O₃ catalysts for possible applications of the Rh/ZrO₂ catalyst developed in the present study to the commercial TWC system. In the double-layered monolith system, the Pd/Al₂O₃ is placed in the bottom of the washcoat and the Rh/ZrO₂ (P) is coated on top of the Pd/Al₂O₃ layer. In the dual-brick monolith system, the Rh/ZrO₂ (P) and Pd/Al₂O₃ monoliths were placed in the front and the rear part of the reactor, respectively. The total monolith length of the dual-brick system is identical to that of the double-layered monolith as listed in Table 3. There are identical amounts of Pd and Rh for all three monolith configurations.

Fig. 9(a) shows the light-off trends of CO, C₃H₆ and NO over the fresh monolith catalysts. The fresh commercial TWC monolith exhibits the lowest T_{50} s for CO and C₃H₆ oxidation and NO reduction, while producing 70 ppm of N₂O at 160 °C probably due to the reduction of NO by C₃H₆, CO and H₂ included in the feed stream [46]. The fresh double-layered and dual-brick monoliths also show high TWC activities, but their T_{50} s for removing CO, C₃H₆ and NO are higher than those of the fresh commercial monolith, as shown in Table 7, probably due to the variety of additives included in commercial monolith [2]. Again, the formation of N₂O is observed over both monoliths at higher temperatures than that over the commercial TWC monolith. No significant difference of T_{50} s has been observed between the double-layered and dual-brick monolith reactors. It is useful to note that under a slightly lean feed condition ($\lambda = 1.01$), the NO conversion can decrease on increasing the reaction temperature in the high temperature region above the reaction light-off temperature during the TWC reaction due to the deficiency of reductants including C₃H₆, CO and H₂ [21,47].

Upon aging, the TWC activities over the monolith reactors decreased dramatically as depicted in Fig. 9(b) and Table 7 for all three reactions. The mechanical strength of the catalyst powder washcoated onto the channels of the monolith reactors has proven to be strong enough to withstand thermal aging without any loss of catalyst powder. For the CO and C₃H₆ oxidation reactions, the light-off curves of all three monoliths shift to higher temperatures upon aging. Among them, the a-dual-brick monolith exhibits the strongest durability with the lowest T_{50} for both reactions. For the double-layered monoliths, the a-commercial monolith shows higher CO and C₃H₆ oxidation activities than the double-layered monolith, probably due to the additive stabilizers in the commercial one [2]. The T_{50} s over the a-dual-brick monolith for the CO and C₃H₆ oxidation reactions are 17 and 36 °C lower than those over both the a-double-layered monoliths including the commercial one, respectively. For the NO reduction reaction, the a-dual-brick monolith is superior to both the aged double-layered monoliths and the commercial one. The a-dual-brick, a-commercial and a-double-layered monoliths also produce around 25 ppm of N₂O at 235, 254 and 273 °C, respectively, where CO and C₃H₆ start their conversions [46]. The a-commercial monolith shows the maximum NO conversions only up to 27% at around 254 °C with its T_{50} unestablished. Similarly, no T_{50} for the a-double-layered monolith can be

determined due to its low NO conversion of less than 30% at the maximum. Gandhi et al. [6,48] reported that the decrease of the deNO_x performance over the double-layered monolith system was caused by the formation of Pd–Rh complex such as metal alloy due to the migration of pure NMs in-between washcoat layers at high reaction temperatures. Since the Rh/ZrO₂ is washcoated in a separate brick in the dual-brick reactor, the formation of Pd–Rh complex by aging may be moderated, resulting in the high efficiency of NO reduction by CO, H₂ and C₃H₆ over the a-Rh/ZrO₂ brick located in the front part of the dual-brick monolith reactor system.

The dual-brick monolith comprised of Rh/ZrO₂ and Pd/Al₂O₃ reveals a much stronger thermal durability than the commercial one containing a number of promoters and/or stabilizers, which may lead to a substantial cost reduction of the modern TWC by adopting the Rh/ZrO₂ as a deNO_x catalyst in combination with the Pd/Al₂O₃ oxidation catalyst.

4. Conclusion

The superior thermal stability of Rh/ZrO₂ has been demonstrated, which strongly depends on the structure of the ZrO₂ supports. ZrO₂ supports having both tetragonal and monoclinic phases have shown better TWC performance and thermal stability than those having the monoclinic phase only. The primary causes for the deactivation of the Rh/ZrO₂ catalyst upon thermal aging include the sintering of Rh and the burial of Rh species into the sublattice region of the ZrO₂ support. Results have indicated that the strong interaction of Rh with the tetragonal ZrO₂ is the key factor preventing the burial of Rh into the sublattice of ZrO₂ over the Rh/ZrO₂s (P and SG). Comparative kinetic studies of TWC reactions have also revealed that the Rh/ZrO₂ catalysts (P and SG) produce the least amount of NH₃ during the course of the TWC reaction among the Rh/metal oxide catalysts examined. Based on these observations, we conclude that the Rh/ZrO₂ is the most promising deNO_x catalyst for application in the advanced TWC system for gasoline engine exhaust. Among the monolith reactor systems comprised of Rh/ZrO₂ (P) and Pd/Al₂O₃, the dual-brick monoliths have shown much stronger thermal durability than the double-layered counterpart, including the commercial one.

Acknowledgments

This work is part of the joint projects, “Development of perovskite-based LNT catalyst and thermally stable TWC” supported by Hyundai-Kia Motors and “National Research Foundation (no. 2011-0029806 “Emission Control Catalytic System for Next Generation Energy-Efficient Vehicle”) of Korea (NRF) grant” funded by the Korea government (MEST).

References

- [1] R.M. Heck, R.J. Farrauto, S.T. Gulati, *Catalytic Air Pollution Control: Commercial Technology*, 2nd ed., John Wiley & Sons, Inc., New York, 2002.
- [2] J. Kašpar, P. Fornasiero, N. Hickey, *Catalysis Today* 77 (2003) 419.
- [3] J.P. Cuif, S. Deutsch, M. Marcz, H.W. Jen, G.W. Graham, W. Chun, R.W. McCabe, *SAE* (1998) 980668.
- [4] J.R. González-Velasco, J.A. Botas, R. Ferret, M.P. González-Marcos, J.-L. Marc, M.A. Gutiérrez-Ortiz, *Catalysis Today* 59 (2000) 395.
- [5] I. Heo, J.W. Choung, P.S. Kim, I.-S. Nam, Y.I. Song, C.B. In, G.K. Yeo, *Applied Catalysis B: Environmental* 92 (2009) 114.
- [6] H.S. Gandhi, G.W. Graham, R.W. McCabe, *Journal of Catalysis* 216 (2003) 433.
- [7] W.B. Williamson, J.C. Summers, J.A. Scaparo, *Catalytic Control of Air Pollution* 3 (1992) 26.
- [8] M. Zimowska, J.B. Wagner, J. Dziedzic, J. Camra, B. Borzecka-Prokop, M. Najbar, *Chemical Physics Letters* 417 (2006) 137.
- [9] H.C. Yao, H.K. Stepien, H.S. Gandhi, *Journal of Catalysis* 61 (1980) 547.
- [10] M. Haneda, O. Houshito, T. Sato, H. Takagi, K. Shinoda, Y. Nakahara, K. Hiroe, H. Hamada, *Catalysis Communications* 11 (2010) 317.
- [11] H. Muraki, G. Zhang, *Catalysis Today* 63 (2000) 337.

- [12] S. Suhonen, M. Valden, M. Hietikko, R. Laitinen, A. Savimäki, M. Härkönen, *Applied Catalysis A-General* 218 (2001) 151.
- [13] Y. Nagai, T. Hirabayashi, K. Dohmae, N. Takagi, T. Minami, H. Shinjoh, S. Matsumoto, *Journal of Catalysis* 242 (2006) 103.
- [14] M. Shane, M.L. McCartney, *Journal of Materials Science* 25 (1990) 1537.
- [15] C. Larese, M.L. Granados, R. Mariscal, J.L.G. Fierro, P.S. Lambrou, A.M. Efstathiou, *Applied Catalysis B: Environmental* 59 (2005) 13.
- [16] H.C. Zeng, J. Lin, W.K. Teo, F.C. Loh, K.L. Tan, *Journal of Non-Crystalline Solids* 181 (1995) 49.
- [17] X. Wu, L. Xu, D. Weng, *Applied Surface Science* 221 (2004) 375.
- [18] J.H. Baik, S.D. Yim, I.-S. Nam, Y.S. Mok, J.-H. Lee, B.K. Cho, S.H. Oh, *Industrial & Engineering Chemistry Research* 45 (2006) 5258.
- [19] P. Avila, M. Montes, E. Miró, *Chemical Engineering Journal* 109 (2005) 11.
- [20] J.H. Baik, H.J. Kwon, Y.T. Kwon, I.-S. Nam, S.H. Oh, *Topics in Catalysis* 42–43 (2007) 337.
- [21] H.J. Kwon, J.H. Baik, S.B. Kang, I.-S. Nam, B.J. Yoon, S.H. Oh, *Industrial & Engineering Chemistry Research* 49 (2010) 7039.
- [22] J.G. Nunan, G.W. Denison, W.B. Williamson, M.G. Henk, SAE PT-123 (2006) 83.
- [23] T. Takeguchi, S. Manabe, R. Kikuchi, K. Eguchi, T. Kanazawa, S. Matsumoto, W. Ueda, *Applied Catalysis A-General* 293 (2005) 91.
- [24] C.E. Hori, H. Permana, K.Y. Simon, A. Brenner, K. More, K.M. Rahmoeller, D. Belton, *Applied Catalysis B: Environmental* 16 (1998) 105.
- [25] M. Boaro, C. Leitenburg, G. Dolcetti, A. Trovarelli, *Journal of Catalysis* 193 (2000) 338.
- [26] T. Bunluesin, H. Cordatos, R.J. Gorte, *Journal of Catalysis* 157 (1995) 222.
- [27] G.W. Graham, H.-W. Jen, W. Chun, R.W. McCabe, *Catalysis Letters* 44 (1997) 185.
- [28] G.W. Graham, H.-W. Jen, W. Chun, R.W. McCabe, *Journal of Catalysis* 182 (1999) 228.
- [29] C.-P. Hwang, C.-T. Yeh, Q. Zhu, *Catalysis Today* 51 (1999) 93.
- [30] J.-M. Li, F.-Y. Huang, W.-Z. Weng, X.-Q. Pei, C.-R. Luo, H.-Q. Lin, C.-J. Huang, H.-L. Wan, *Catalysis Today* 131 (2008) 179.
- [31] L. Marot, R. Schoch, R. Steiner, V. Thommen, D. Mathys, E. Meyer, *Nanotechnology* 21 (2010) 365707.
- [32] M.D. Villalpando, D.A. Berry, T.H. Gardner, *International Journal of Hydrogen Energy* 33 (2008) 2695.
- [33] S. Eriksson, S. Rojas, M. Boutonnet, J.L.G. Fierro, *Applied Catalysis A-General* 326 (2007) 8.
- [34] P. Fornasiero, R. Di Monte, G. Ranga Rao, J. Kašpar, S. Mweriani, A. Trovarelli, M. Graziani, *Journal of Catalysis* 151 (1995) 168.
- [35] J. Fan, X. Wu, X. Wu, Q. Liang, R. Ran, D. Weng, *Applied Catalysis B: Environmental* 81 (2008) 38.
- [36] R.C. Garvie, *Journal of Physical Chemistry* 82 (1978) 219.
- [37] K.T. Jung, Y.G. Shul, A.T. Bell, J. Korean, *Chemical Engineering* 181 (2001) 992.
- [38] Z. Weng-Sieh, R. Gronsby, A.T. Bell, *Journal of Catalysis* 170 (1997) 62.
- [39] Y.-C. Zhang, R. Kershaw, K. Dwight, A. Word, *Journal of Solid State Chemistry* 72 (1988) 131.
- [40] Y.-C. Zhang, K. Dwight, A. Word, *Materials Research Bulletin* 21 (1986) 853.
- [41] R.H. French, S.J. Glass, F.S. Ohuchi, Y.-N. Xu, W.Y. Ching, *Physical Review B* 49 (1994) 5133.
- [42] K.-H. Jacob, E. Knözinger, S. Benier, *Journal of Materials Chemistry* 3 (1993) 651.
- [43] J.M. Grau, J.C. Yori, C.R. Vera, F.C. Lovey, A.M. Condó, J.M. Parera, *Applied Catalysis A-General* 265 (2004) 141.
- [44] L.S. Escandón, S. Ordóñez, F.V. Díez, H. Sastre, *Reaction Kinetics Catalysis Letters* 76 (2002) 61.
- [45] W. Li, K. Perry, K. Narayanaswamy, C. Kim, P. Najt, DEER Conference (2009).
- [46] P. Granger, V.I. Parvulescu, *Past and Present in DeNO_x Catalysis from Molecular Modeling to Chemical Engineering*, 1st ed., Elsevier, The Netherlands, 2007.
- [47] S.B. Kang, H.J. Kwon, I.-S. Nam, Y.I. Song, S.H. Oh, *Industrial & Engineering Chemistry Research* 50 (2011) 5499.
- [48] G.W. Graham, H. Sun, W.-W. Jen, X.Q. Pan, R.W. McCabe, *Catalysis Letters* 81 (2002) 1.